Dipolar coupling between electronic transitions of the DNA bases and its relevance to exciton states in double helices

B. Bouvier, T. Gustavsson, D. Markovitsi[*], P. Millié[*]

Laboratoire Francis Perrin (CNRS FRE 2298), SPAM, CEA Saclay, F-91191 Gif-sur-Yvette, France

Abstract

The present communication addresses the question of the magnitude of dipolar coupling between the lowest electronic transition moments of the DNA nucleosides and its relevance to Frenkel exciton states in double helices. The transition energies and moments of the nucleosides are determined from absorption spectra recorded for dilute water solutions. Dipolar interactions are computed for some typical nucleoside dimers according to the atomic transition charge distribution model. The properties of the exciton states of two particular double helices, $(dA)_{20} \cdot (dT)_{20}$ and $(dAdT)_{10} \cdot (dAdT)_{10}$, are calculated considering three closely lying molecular electronic transitions (S_1 and S_2 for adenosine, S_1 for thymidine). It is shown that (i) the oscillator strength is distributed over a small number of eigenstates, (ii) important mixing of the three monomer electronic transitions may occur, (iii) all eigenstates are spatially delocalised over the whole length of the double helix and (iv) the extent of exciton states over the two strands depends on the base sequence. © 2002 Elsevier Science B.V. All rights reserved.

1. Introduction

Various photoreactions occurring upon absorption of UV irradiation by the DNA bases (adenine, cytosine, guanine and thymine) are known to have lethal or mutagenic effects on the cells [1]. The yield of such photoreactions may be enhanced if they are preceded by a transport process (charge or electronic excitation energy) within the double helix. In view of the crucial role the transport phenomena can play in the appearance of skin cancers, it is important to elucidate the associated mechanisms. Indeed, the study of charge transport in DNA has recently found a renaissance with the support of ultrafast spectroscopy and sophisticated theoretical calculations [2]. In contrast, such means have not yet been used to improve our understanding of energy migration in DNA for which no clear picture has emerged so far in spite of the efforts made for more than thirty years [3–8].

The main controversial point is whether the excited states involved in singlet excitation migration are localised on just one base or whether they extend over a certain number of them. The exciton theory has been used since the early sixties in the

---

[*] Corresponding authors. Tel.: +33-1-6908-4644; fax: +33-1-6908-8707.

E-mail addresses: dmarkovitsi@cea.fr (D. Markovitsi), millie@pandora.saclay.cea.fr (P. Millié).
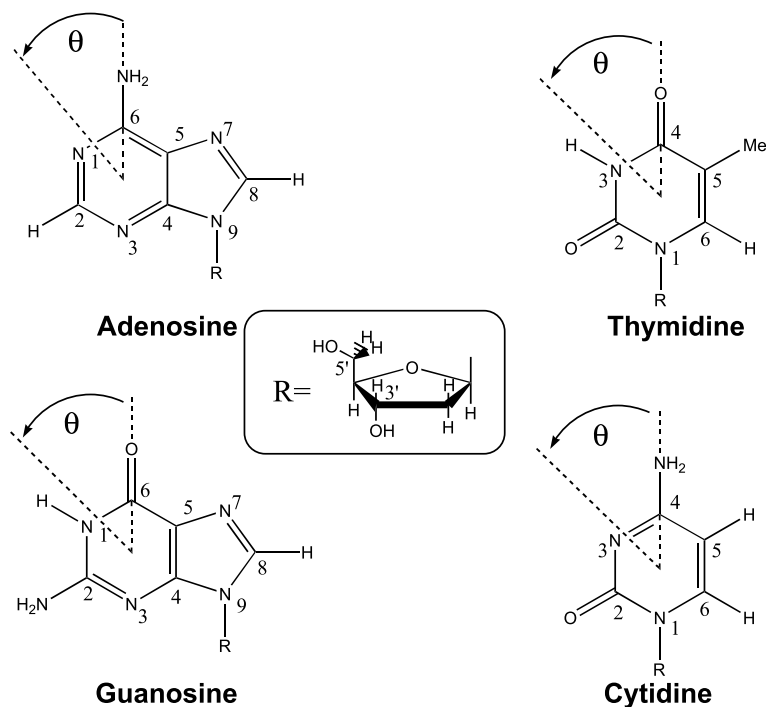
Fig. 1. The studied nucleosides: adenosine (dA), cytidine (dC), guanosine (dG) and thymidine (dT). In the quantum chemistry calculations the deoxyribose residue is replaced by a methyl group. The angle θ denotes the direction of the transition moments.

analysis of the DNA electronic excited states [9–12]. Some authors draw the conclusion that the excited states remain localised since exciton splitting is not observed upon formation of the double helix [13]. This type of reasoning has also guided most of the "experimental" [1] investigations [3–8] of singlet energy migration where the photosensitised fluorescence from an energy trap is analysed in terms of excitation hopping via a Förster mechanism [14].

This controversy arises from the complexity of the system and is related to both theoretical and experimental difficulties, as well as to conceptual problems. Below, we enumerate some of them and we comment on the possibility of overcoming them. In what follows we use the term "chromophore" to denote the nucleosides, deoxyadenosine (dA), deoxycytidine (dC), deoxyguanosine (dG) and deoxythymidine (dT), composed of a base and

the deoxyribose residue (Fig. 1). Their optical properties differ from those of the bases but they are quite similar to those of nucleotides which are the monomeric units of nucleic acids [15,16].

1. The lowest absorption bands of the four nucleosides are very broad; they all peak in the same spectral region (260–270 nm) and they have similar intensities [15,16]. Moreover, fluorescence anisotropy and circular dichroism measurements have revealed that the adenosine and guanosine absorption bands correspond to more than one electronic transition [17–19]. Thus, it would in principle be possible to improve the modelling of electronic excitations in double helices by using experimental values of transition energies and transition moments of individual chromophores resulting from a more refined spectral analysis.

2. Since the excitation energy, the transition moment and the polarisation of the dipolar transitions are specific to each type of nucleoside, the collective properties of the double helices are expected to depend on the base sequence. Therefore,

---

[1] In the sense that they are model dependent.

a study of energy migration at the molecular level can only be performed for double helices with known base sequence and not for native DNA. The base sequence effect on the energy transfer efficiency to an energy trap has been experimentally evidenced for double-stranded decamers [20,21].

3. In most calculations of the DNA exciton states, the dipolar coupling between electronic transition moments was calculated by means of the point dipole approximation. This approximation is also implicit in the Förster formula [14] used in the "experimental" studies approaching energy migration as a hopping process. One would expect this approximation not to be valid for double helices where the interchromophore distance is of the same order of magnitude as the chromophore dimensions, as already pointed out in 1969 by Miyata and Yomosa [12]. The electronic coupling can be calculated in a much more accurate way using the method of atomic transition charges [12,22,23].

4. In all the studies dealing with DNA exciton states and energy migration in double helices, not only may the dipolar coupling be unsatisfactorily described but interactions due to orbital overlap are also neglected. Among these interactions, charge resonance and charge transfer terms may become important when the strength of dipolar transitions decreases [24–26]. In particular, these interactions are involved in the formation of excimers and exciplexes often invoked in discussions on nucleic acid components [27–31].

5. The strength of the electronic coupling responsible for the formation of collective excited states and excitation transport may be seriously affected by structural disorder. Various types of conformations are known to occur in double helices in solution. They depend on the base sequence and can be simulated using molecular modelling [32].

6. We have seen in point 2 that it is important to work with double helices with known base sequence so as to correctly model the excited states and the excitation transport. The experimental counterpart resides in the difficulty of obtaining well-defined double helices in solution. Although polynucleotides of known base sequence are commercially available, the pairing of comple-

mentary single strands may lead to mismatching. Structural characterisations have to be carried out before the photophysical properties measured can be unambiguously attributed to double-stranded helices.

7. Another serious experimental difficulty when working with nucleic acids is the low-fluorescence quantum yields [33] and the extremely short lifetimes of the singlet excited states [34,35]. Only recently has femtosecond transient absorption spectroscopy been used to study the photophysical properties of bases and nucleosides [36,37].

Within this context we have undertaken a study aimed at a better understanding of electronic excitations in polynucleotide double helices using methodologies we previously developed for the investigation of exciton states and excitation transport in columnar phases [23,26,38,39]. The present communication is our first approach to this problem. Our efforts are focused on the improvement of the points 1 to 3 mentioned above, e.g., use of accurate properties for chromophore transition moments, consideration of oligomers with given base sequence and calculation of dipolar coupling by means of the atomic transition charges.

Firstly, we determine the properties of the individual chromophores in the double helices. Experimentally, we record the absorption spectra of nucleosides in dilute water solutions to avoid aggregation. Using fluorescence anisotropy data from the literature [17,19], we determine the energy and the transition moments of the lowest electronic transitions. In parallel, we calculate these properties with the conformation spectra–intermediate neglect of differential overlap–configuration interaction by perturbative selected iterations (CS–INDO–CIPSI) method and we compare the results to both our experimental data and to the results of calculations as reported in the literature (Section 3).

Secondly, we are interested in the magnitude of dipolar coupling encountered in some typical dimers, both stacked and paired, as was recently done for the electronic coupling responsible for charge transport [40]. We compare the results obtained using the atomic transition charge distribution model with those calculated by means of

the point dipole approximation. Moreover, we examine whether it is possible to determine, for each nucleoside, a dipole length so that the extended dipole approximation [41], convenient for simulations, can be used to correctly describe the dipolar coupling in double helices (Section 4).

Thirdly, we calculate the properties of the exciton states for two simple DNA oligomers, each one consisting of twenty identical dA–dT pairs, by considering two electronic transitions for adenosine and one for thymidine. The two types of nucleosides are either located on different strands $(dA)_{20} \cdot (dT)_{20}$, or alternate in the same strand $(dAdT)_{10} \cdot (dAdT)_{10}$. We examine the energy, the oscillator strength and describe the spatial and electronic delocalisation of each eigenstate. Finally, we illustrate the topography of some typical eigenstates by representing the contribution of the electronic transitions of each particular nucleoside to these collective states (Section 5).

2. Methods

2.1. Experimental procedure

Nucleosides were purchased from Sigma Aldrich and used without further purification. They were dissolved in ultrapure water produced by a Millipore (Milli-Q) purification system. Absorption spectra were recorded in the UV region down to 200 nm with a Perkin Lamda 900 spectrophotometer using 1 and 5 cm quartz cells.

The spectral analysis was performed by using PeakFit software (Jandel Inc.). Each spectrum was decomposed into a sum of sub-bands. Each sub-band was represented by a log-normal function according to the equation:

$$\varepsilon(v) = \varepsilon_0 \exp \left[- \frac{\ln(2)\left[\ln\left(\frac{(v-v_0)(\gamma^2-1)}{\gamma\,\Delta v} + 1\right)\right]^2}{[\ln\gamma]^2} \right], \tag{1}$$

where ε_0 is the maximum value of the molar extinction coefficient, v_0 the position of the absorption maximum, Δv the full width at half maximum

(FWHM) of the absorption band and γ the asymmetry parameter. It has been shown that a log-normal curve better describes an asymmetric structureless absorption band than a gaussian one [42].

The oscillator strengths f and the transition moments μ (in Debyes) corresponding to a given log-normal curve were calculated according to the equations:

$$f = 4.317 \times 10^{-9} A, \tag{2}$$

$$\mu^2 = 9.181 \frac{A}{v_0} \times 10^{-3}, \tag{3}$$

where $A = \int_{-\infty}^{\infty} \varepsilon(v)\,dv$ is the integral of the absorption band (in $l\,mol^{-1}\,cm^{-2}$) and v_0 is the peak transition energy (in cm^{-2}).

2.2. Calculation procedure

2.2.1. General formalism

The excited states of double-stranded DNA fragments are calculated in the framework of the exciton theory [43–45], in which the exact Hamiltonian of an *n*-molecular supersystem may be written:

$$H = H_0 + V. \tag{4}$$

H_0, the unperturbed Hamiltonian of the supersystem, is evaluated as the sum of the individual Hamiltonians of the isolated molecules. As a consequence, zeroth-order eigenfunctions of the system consist of products of the eigenfunctions of these molecules:

$$H_0 = \sum_{\text{molecules}, k}^{n} H_k \quad \text{and} \quad \left|\Phi_m^i\right\rangle = \Psi_m^i \prod_{\text{molecules}, k \neq m}^{n} \Psi_k^0, \tag{5}$$

where Ψ_m^i denotes the *i*th excited state of chromophore *m*. The excited states of the supersystem are thus decomposed on states for which the excitation is localised on a given monomer, the other molecules being in their respective ground states.

V is the perturbation operator, which was formalised by Longuet-Higgins [46] using a local charge density operator $\rho^{(k)}(\vec{r}^{(k)})$ associated with each individual chromophore *k*:

$$V = \int \int \frac{\rho^{(k)}(\vec{r}^{(k)})\rho^{(l)}(\vec{r}^{(l)})}{|\vec{r}^{(k)} - \vec{r}^{(l)}|} \, d\vec{r}^{(k)} \, d\vec{r}^{(l)}. \qquad (6)$$

Since these operators depend exclusively on the coordinates of the individual subsystems, separation of variables inside the integrand yields, as an expression of the general matrix element of V:

$$\langle \Psi_n^i \Psi_m^j | V | \Psi_n^k \Psi_m^l \rangle =$$
$$\frac{\langle \Psi_n^i | \rho^{(n)} \vec{r} | \Psi_n^k \rangle \langle \Psi_m^j | \rho^{(m)} \vec{r} | \Psi_m^l \rangle}{|\vec{r}^{(n)} - \vec{r}^{(m)}|} \, d\vec{r}^{(n)} \, d\vec{r}^{(m)}. \qquad (7)$$

This expression may be viewed as an interaction between appropriate transition charges which can be calculated at different levels of approximation (point dipoles, extended dipoles, atomic transition charges,...).

The placement of a point dipole on a molecule devoid of inversion centre (such as the DNA bases) is problematic. Moreover, this approximation is inappropriate when the interchromophore distance is of the same magnitude as molecular dimensions. In such cases, the extended dipole approximation [41] is traditionally used. An electronic transition at this level of approximation is represented by two opposite charges $+q$ and $-q$ separated by a distance l, such that $\vec{\mu} = q\vec{l}$, where μ is the transition moment.

In the atomic transition charges model, the off-diagonal terms are subjected to a dipolar development [47]. The resulting molecular transition dipoles $\vec{\mu} = \langle \Psi_m^k | \vec{r} | \Psi_m^0 \rangle$ are then decomposed onto the atomic orbitals of the molecule, in the framework of the INDO approximation [48]. This treatment yields transition charges located on each atom of the molecule, as well as local transition dipoles whose contribution is generally negligible for $\pi \rightarrow \pi^*$ transitions (typically $\approx 5\%$). The dipole moment associated with the charge distribution is approximately equal to the corresponding transition moment.

At the first order of perturbation, consideration of the expression of the total electronic Hamiltonian H in the basis formed by the eigenfunctions of H_0 is sufficient. Diagonalisation of the matrix yields N eigenstates

$$\Phi_k = \sum_{\text{molecules } m} \sum_{\text{states } i} C_{k,m}^i | \Psi_1^0 \Psi_2^0 \cdots \Psi_m^i \cdots \Psi_n^0 |. \qquad (8)$$

The transition moments associated with the eigenstates are given by:

$$\vec{\mu}_k = \sum_{\text{molecules } m} \sum_{\text{states } i} C_{k,m}^i \vec{\mu}_m^i. \qquad (9)$$

Eq. (9) implies that the model is conservative with regard to μ^2: the sum of squared transition moments of the monomers equals the sum of squared eigenstate transition moments.

The localisation behaviour of the eigenstates is usually expressed by the inverse participation ratio L_k [49,50]. The number of coherently coupled chromophores in a given eigenstate k is given by the participation ratio $1/L_k$. When the eigenstates are built on more than one molecular states, L_k is written as [23]:

$$L_k = \sum_{\text{molecules } m} \left[\sum_{\text{states } i} (C_{k,m}^i)^2 \right]^2. \qquad (10)$$

An interesting comparison can be drawn between the exciton theory and direct calculation of the excited states of the supersystem as a whole. At the lowest level of complexity, a configuration interaction (CI) restricted to singly excited configurations (CIS) is applied, on the one hand, to each monomer sub-unit and followed by an exciton treatment, and on the other hand, to the entire supersystem. These two treatments are equivalent under the following conditions: (i) the perturbation is sufficiently small, (ii) the basis used consists of molecular orbitals that are localised on each molecule, and (iii) orbital overlap interactions (exchange, charge resonance, charge transfer) are small compared to Coulombic interactions. Conversely, Eq. (5) implies complete neglect of orbital overlap interactions.

Alternately, transition charges can be obtained using a higher level of theory than a CIS. Direct treatment of the excited states of the supersystem at this same level is often tedious or unfeasible, whereas the exciton theory yields correct results if the previous three conditions are fulfilled. An important difference between the two aforementioned approaches concerns the modelling of the well-known DNA hypochromism [51], that is, the decrease in intensity of the absorption spectrum upon pairing of two single strands resulting in the

formation of the double helix. The supersystem CIS method accounts for hypochromism [52] most probably because it includes charge transfer excitations, in contrast to our approach which we deem unable to reproduce this phenomenon. Tinoco's [9,11] explanation of hypochromism based on the exciton theory, already criticised by Rhodes [10], can be attributed to a large number of approximations, particularly an overestimation of the off-diagonal terms due to the use of the point dipole model (cf. Section 4).

2.2.2. Computational details

The deoxynucleosides were modelled by the corresponding 9-methylated purines or 1-methylated pyrimidines and described by their most abundant tautomeric form (Fig. 1). Their geometry was optimised at the AM1 level. So as to allow separation of the σ and π subsystems in the INDO treatment, and in agreement with calculations on the isolated bases [53], the heavy atom skeletons were kept planar (point group C_s) during the optimisation process. Rotation of the substitutive methyl group around the N1–C or N9–C bond axis was also optimised. The geometry of the two Watson–Crick base pairs dG–dC and dA–dT were derived from those of the individual bases; relative placement parameters were taken from [54]. Positioning of the pseudo-dyad followed conventions described in Ref. [55]. For the calculation of coupling elements between all possible base pairs, a standard B-DNA geometry was generated from the Watson–Crick pairs (36° twist, 3.4 Å rise) [54], regardless of the bases considered. The oligonucleotides $(dA)_{20} \cdot (dT)_{20}$ and $(dAdT)_{10} \cdot (dAdT)_{10}$ were built using a standard B-DNA geometry. Sequence dependent changes in helical twist and rise were taken from X-ray diffraction studies on fibres [56] and single crystals [57]: 36° twist and

3.29 Å rise for $(dA)_{20} \cdot (dT)_{20}$, 31°/41° twist and 3.34 Å rise for $(dAdT)_{10} \cdot (dAdT)_{10}$. The sugar-phosphate backbones of DNA helices were not taken into account.

For the calculation of dipolar coupling, computed transition moments were rescaled so as to coincide with experimental values, whereas transition moment directions were those determined according to the atomic transition charges model. Diagonal elements of the exciton matrix were taken equal to the experimental excitation energy (Table 1). Successive transitions on the same purine were considered orthogonal to each other. Interactions were not restricted to nearest neighbours: all the off-diagonal matrix elements were evaluated.

The extended dipole for a given transition was positioned along the axis defined by the weighted centres of negative and positive atomic transition charges. It was placed at the weighted centre of the absolute values of the atomic transition charges. The values of charge q and distance l were chosen so as to verify the following conditions: (i) $\mu = ql$, μ being the experimental transition dipole moment, and (ii) the coupling matrix elements calculated on the basis of the interaction between two extended dipoles is equal to that calculated with the atomic transition charges model, for two superposed identical DNA bases whose planes of symmetry are parallel and separated by a distance of 3.5 Å. These two conditions uniquely define parameters q and l.

The σ subsystem on each chromophore was localised on individual bonds, whereas the π subsystem was allowed to delocalise over the whole molecule. The subsequent CI was not limited to monoexcitations or to the π and π^* molecular orbitals, so as to ensure a better description of differential correlation effects and σ system

Table 1

Energy (cm^{-1}) and transition moment (D) of the three lowest singlet electronic transitions of nucleosides deduced from the experimental absorption spectra in 10^{-5} M water solutions

	dA[a]	dC	dG	dT
$S_0 \rightarrow S_1$	36 700 (1.60)	36 800 (3.45)	36 700 (3.31)	37 500 (3.68)
$S_0 \rightarrow S_2$	38 800 (3.70)	42 100 (2.18)	40 300 (3.31)	46 600 (2.75)
$S_0 \rightarrow S_3$	45 500 (1.20)	44 900 (2.22)	48 200 (2.44)	49 900 (1.63)

[a] From Ref. [19].

reorganisation. Individual $\sigma_i \rightarrow \sigma_j^*$ transitions were allowed to contribute as long as molecular orbitals i and j share a common atomic centre. This approach typically accounts for 95% of the correlation energy. Resulting configurations were then sorted with regard to their weight, in the framework of the CIPSI [58] algorithm, and yielded a CI matrix containing five to ten thousand individual configurations. The wave functions generated by diagonalisation of the CI matrix were used to determine atomic transition charges, as well as transition dipole moments associated with each excited state.

3. Individual chromophores

In this Section, we focus on the electronic transitions of individual chromophores on which the magnitude of dipolar coupling and the properties of exciton states depend. The transition energies and the transition moments are obtained from the experimental absorption spectra, whereas transition directions and atomic transition charges are calculated using the CS–INDO–CIPSI method, whose validity is checked by comparing the experimental and calculated values of transition energies and transition moments. As a wealth of theoretical information about the electronic transitions of the nucleic acid bases has been gathered over the years, we also compare our theoretical data with selected literature results.

Fig. 2 shows the absorption spectra of the four nucleosides obtained for 10^{-5} M concentrations. We found that at higher concentrations the Beer–Lambert law is not obeyed. The concentration dependence of the photophysical properties of nucleosides will be the object of a forthcoming communication. The spectrum profiles in Fig. 2 resemble those reported in the literature and the molar extinction coefficients match within 10% the reported values, for which the concentrations are not mentioned [15,16].

We performed a decomposition of each spectrum into sub-bands in the region 30 000–50 000 cm^{-1} according to the fitting procedure described in Section 2.1. All the log-normal curves used to fit each spectrum were constrained to have the same
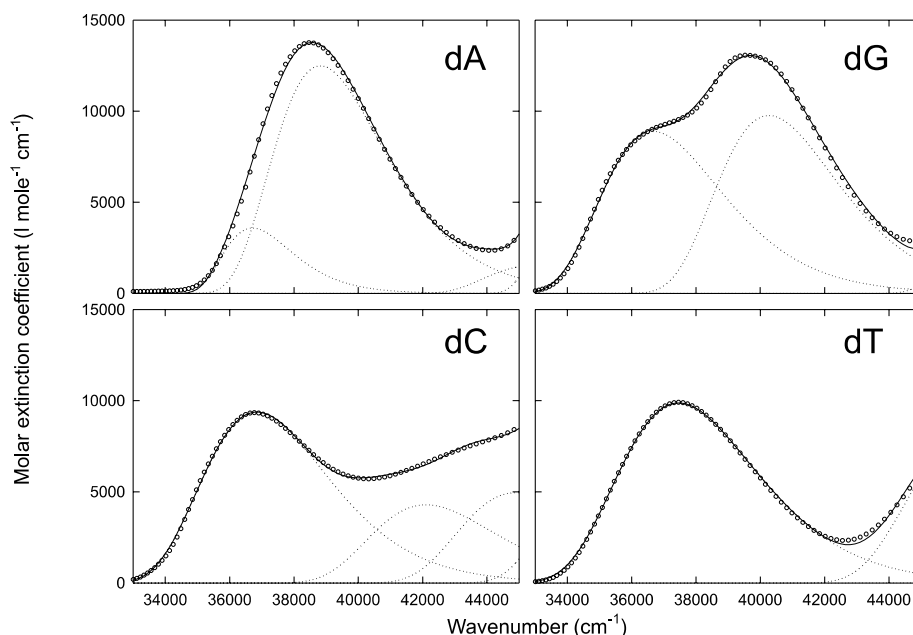

Fig. 2. Absorption spectra (circles) of the adenosine, cytidine, guanosine and thymidine in ultrapure water (10^{-5} M) fitted with a sum (solid lines) of log-normal curves (dotted lines).

width and we used the minimum number of curves giving an acceptable fit. Although our decomposition is phenomenological, we based it on fluorescence anisotropy and linear dichroism measurements reported in the literature. These measurements suggest that the lowest absorption band corresponds to a single electronic transition for cytidine and thymidine whereas that of adenosine and guanosine is an envelope of two transitions with different polarisations [17]. For adenosine, we fixed the first two transition energies to the values given in a recent detailed analysis [19], and allowed the first weak transition to be slightly narrower.

The resulting fitted curves are shown as solid lines in Fig. 2. As can be seen, the description is fully satisfactory. The sub-bands above 42 000 cm^{-1} are only included to stabilise the description of the lowest transitions and are not further treated in the present paper. The numerical results of the fits for the three lowest transitions are shown in Table 1. In what follows, we will consider only one

transition for cytidine and thymidine and two for adenosine and guanosine. This choice is made because the other transitions are too high in energy and/or they have a weak transition moment. Therefore, they are not expected to mix with the lower ones within the same exciton band.

Experimental and calculated values of transition energies, along with associated directions and oscillator strengths, are compiled in Tables 2 and 3 for purines and pyrimidines, respectively. Transition moment directions, visualised by means of the angle θ [59] (Fig. 1), are taken from the literature [19,60–62]. Selected literature results based on semi-empirical methods [53,63–65] and more recent studies based on ab initio calculations [53,66–69] are presented in the same Tables.

The theoretical and experimental values are in good agreement as far as excitation energies and oscillator strengths are concerned. The oscillator strength of cytidine is rather underestimated, probably because the global parameterisation of the CS–INDO method is not as well adapted for

Table 2

Energy (cm^{-1}), oscillator strength and directions of the two lowest electronic transitions of purines. Comparison with literature data

Method/level	$S_0 \to S_1$			$S_0 \to S_2$		
	E	f	θ^a	E	f	θ^a
Adenosine						
CS–INDO	37 175	0.057	+1	39 840	0.216	+52
Experiment (Section 2.1)	36 700	0.05	+66[b]	38 800	0.24	+19[b]
INDO/S[c]	35 714	0.099	+30	38 168	0.305	+62
Rescaled CIS/6-31 G*[d,e]	37 100	0.41	+38	37 500	0.03	−72
Ab initio MRCI[d,f]	36 400	0.001	−33	38 600	0.318	+41
CASPT2[d,e]	38 100	0.236	+43	38 200	0.001	−56
Guanosine						
CS–INDO	34 245	0.232	−57	40 160	0.203	+54
Experiment (Section 2.1)	36 700	0.19	−4/35[g]	40 300	0.21	−75[g]
INDO/S[h]	31 750	0.28	−44	36 300	0.38	+57
Rescaled CIS/6-31 G*[d,e]	35 600	0.29	−46	40 300	0.50	+63
Ab initio MRCI[d,f]	36 200	0.20	−64	42 700	0.09	+52
CASPT2[d,i]	35 842	0.24	−52	36 900	0.09	+3

[a] See Fig. 1.
[b] From Ref. [19].
[c] From Ref. [63].
[d] Values corresponding to 9H-purine.
[e] From Ref. [53].
[f] From Ref. [66].
[g] From Ref. [61].
[h] From Ref. [65].
[i] From Ref. [68].

Table 3
Energy (cm^{-1}), oscillator strength and directions (Fig. 1) of the two lowest electronic transitions of pyrimidines—comparison with literature data

Method/level	$S_0 \rightarrow S_1$		
	E	f	θ^a
Thymidine			
CS–INDO	36 360	0.220	−13
Experiment (Section 2.1)	37 500	0.24	+14/−19[b]
CNDO/OPTIC-2[c]	39 200	0.245	+14
Rescaled CIS/6-31 G*[d,e]	41 100	0.36	−3
CASPT2[d,f]	39 400	0.17	+15
Cytidine			
CS–INDO	36 100	0.102	+38
Experiment (Section 2.1)	36 800	0.21	+9/+51[g]
INDO/S[e]	31 750	0.28	−44
Rescaled CIS/6-31 G*[d,e]	35 600	0.29	−46
CASPT2[d,h]	36 200	0.20	−64

[a] See Fig. 1.
[b] From Ref. [60].
[c] From Ref. [63].
[d] Values correspond to 1H-pyrimidines.
[e] From Ref. [53].
[f] From Ref. [67].
[g] From Ref. [62].
[h] From Ref. [69].

this particular chromophore as for the others. Nevertheless, the overall accord between both sets of results justifies the rescaling of transition moments explained in Section 2.2.2. At this point, it is interesting to compare our data with these obtained by Miyata and Yomosa who studied exciton states of oligonucleotides [12]. The atomic transition charges derived by these authors from a limited CIS calculation [70] of the bases lead to important errors in the oscillator strength values and to state inversions.

A vast number of semi-empirical methods, reviewed in Ref. [18], have been utilised, ranging from INDO/S to CNDO or MNDO. These calculations are based on CI between singly or singly and doubly excited states. As a rule, they have proved able to reproduce most experimental transition energies and oscillator strengths, but generally fail to provide consistent transition moment directions. Discrepancies in results between different methods may be attributed to varying parameterisations. The necessity to include at least doubly excited states in the CI space to ensure

correct treatment of conjugated molecules, such as the DNA bases, has been pointed out by Volosov [63].

Correct ab initio treatment of transition energies and moments requires to take into account the variation of the dynamic correlation between the ground and excited states. Energy calculations that meet this requirement can be achieved using the CASPT2 method. The choice of the active space at the CASSCF level determines the quality of the zeroth-order wave function used for CASPT2; as a consequence, CASPT2 results for near-degenerate excited states may not prove satisfactory, as is the case for the first two $\pi \rightarrow \pi^*$ transitions of adenine. These transitions, clearly separated at the CASSCF level, are rendered almost degenerate by the PT2 correction [53]. Ab initio CIS, although less computationally expensive, takes no heed of differential correlation effects nor of the σ system's reorganisation. Hence, results obtained at this level need to be rescaled, considering the difference in electronic correlation between the ground and excited states as a constant. Furthermore, CIS calculations do not correctly describe excited states possessing a substantial doubly excited character or multiconfigurational structure, for which CASSCF, MCSCF or MRCI methods are better suited.

On the whole, a relatively good agreement between different quantum chemistry methods as well as between theory and with experiment can be noted for the energies and oscillator strengths of the first few $\pi \rightarrow \pi^*$ states of the methylated DNA bases. This is not the case concerning transition moment directions, which still lack reliability; experimental determinations of these directions may also be rather imprecise, rendering comparison with experiment somewhat troublesome. In particular, the transition moment directions of 9-methylguanine are very similar at every level of theory but blatantly disagree with the values reported by experimentalists.

4. Dipolar coupling

In this Section, we present the atomic transition charge distributions for the four nucleosides,

which we apply to the determination of the dipolar coupling. Using this sophisticated formalism as a reference, we test the validity of the point dipole and the extended dipole approximations for geometries generated by simple spatial transformations (translations and rotations). Finally, we determine intrastrand and interstrand coupling elements for nearest neighbours in typical B-DNA structures.

The calculated transition monopoles on the atomic centres of the methylated bases are schematised in Fig. 3. As can be seen, the first transition of both purines is rather localised on the six-membered ring, in contrast with the more delocalised character of the second transition for which the role of the transition monopole on atom C8 is notably increased. The substituent methyl groups do not carry significant charge and probably do not influence transition moment directions or intensities as far as the first two transitions on each purine are concerned. This is in agreement with the theoretical finding [64] that differently substituted adenines and guanines are characterised by similar transition charge distributions. In addition, the monopole decomposition presented in Fig. 3 is very similar to that reported by these
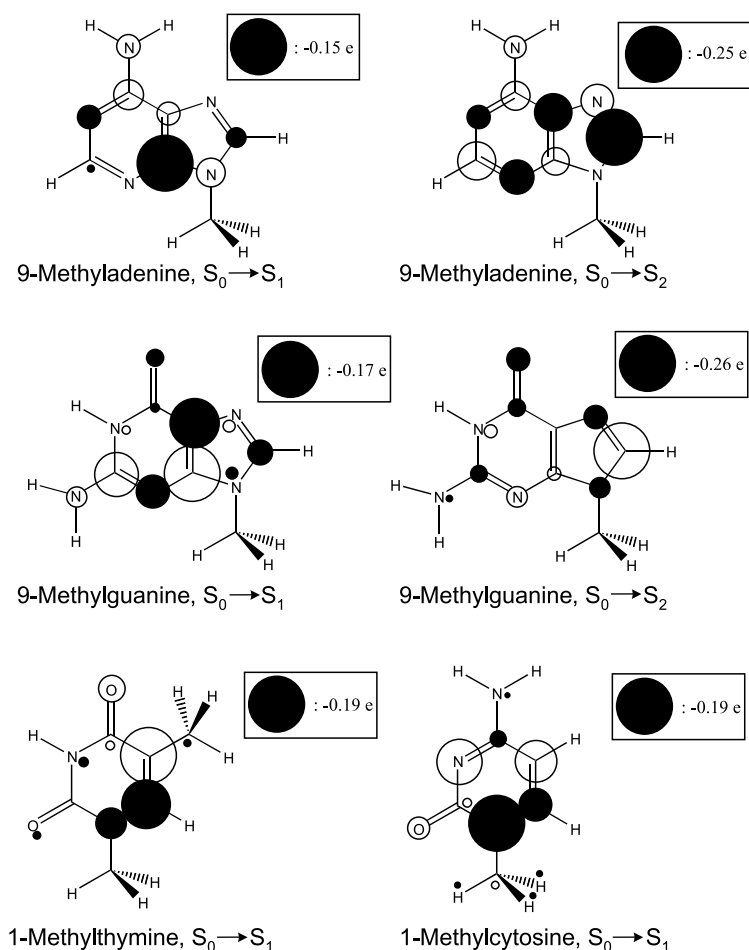

Fig. 3. Atomic transition charges found for the methylated DNA bases according to the CS–INDO–CIPSI method. Full circles correspond to negative charges and empty circles to positive charges; the circle diameter is proportional to the absolute value of the charge.

authors on the basis of the CNDO/OPTIC-2 semi-empirical method. The influence of carbonyl and amino groups on the transition moments may also be considered rather unimportant, as can be seen when comparing transition charge distributions on 1-methylthymine and 1-methylcytosine.

Table 4 presents the values of the extended dipole length l and the associated charge q, calculated as described in Section 2.2. We remark that values of l roughly correspond to typical dimensions of the part of the nucleoside concerned by the excitation. Furthermore, they are of the same order of magnitude compared to nearest-neighbour distances in double helices, justifying a priori the inadequacy of the point dipole model outlined further in this study.

The values of dipolar coupling V calculated at three levels of approximation are compared in Fig. 4 for two stacked and parallel thymidine chromophores, as a function of the stacking distance R. For clarity, we show the values of V scaled by R^3, giving a constant value for the point dipole model. The agreement between the atomic transition charges and the extended dipole models is remarkable at every distance. For values of R superior to 20 Å, both plots behave asymptotically and tend towards the point dipole curve. For stacking distances found in DNA (3.4 Å), the point dipole approximation results in a threefold error.

The aforementioned good performance of the extended dipole is understandable given the way in which q and l are defined (Section 2.2). The robustness of the approximation can be further tested by relative rotation of two chromophores around the helical axis. The result obtained for two cytidine chromophores is shown in Fig. 5. As the rotation angle increases, we observe that the values of dipolar coupling computed according to
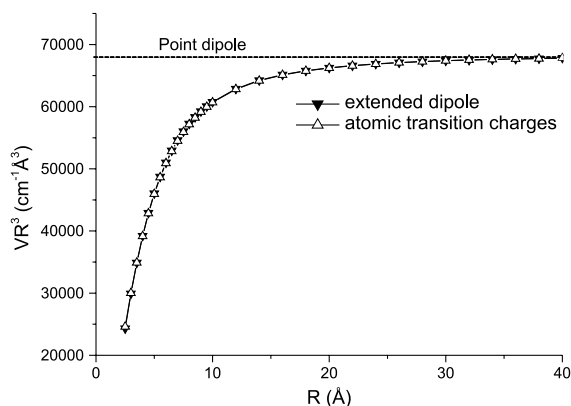

Fig. 4. Dipolar coupling V between the $S_0 \rightarrow S_1$ transition moments of two stacked and parallel thymidine chromophores as a function of the stacking distance R calculated according the point dipole (dashed line), the extended dipole (filled triangles) and the atomic transition charges (empty triangles) formalisms.

the extended dipole model diverge from those taken as reference. The dipolar interaction at 36°, typical of B-DNA, exhibits an error of $\approx 100\%$. Similar inaccuracies have been noted for other nucleoside dimers.

We have shown earlier that the extended dipole model yields quite similar results to atomic transition monopoles for triphenylene derivatives stacked in columnar phases and allowed to rotate around the column axis [23]. In this case, the chromophores have a centre of symmetry which coincides with the rotation axis. By contrast, chromophores in double helices are devoid of an inversion centre and are rotated around an off-centred axis. Hence, the extended dipole cannot account for varied relative positions of the monomers, due to its lack of theoretical foundations.

Given the insufficiencies of the point dipole and extended dipole models, we apply the atomic

Table 4
Extended dipole length l (Å) and absolute value of charges q (e) associated with the electronic transitions of nucleosides

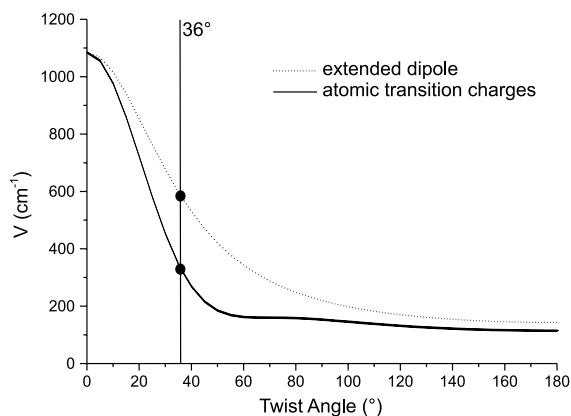|	Adenosine		Thymidine	Guanosine		Cytidine
	$S_0 \rightarrow S_1$	$S_0 \rightarrow S_2$	$S_0 \rightarrow S_1$	$S_0 \rightarrow S_1$	$S_0 \rightarrow S_2$	$S_0 \rightarrow S_1$
q	0.15	0.16	0.19	0.15	0.16	0.28
l	2.32	4.63	4.10	4.72	4.24	2.53

Fig. 5. Dipolar coupling V between the $S_0 \rightarrow S_1$ transition moments of two cytidine chromophores located in parallel planes distant of 3.4 Å as a function of the twist angle calculated according to the extended dipole (dotted line) and the atomic transition charge (continuous line) formalisms. The full circles denote the coupling corresponding to a twist angle of 36°, typical of B-DNA.

transition charges model to the computation of coupling elements between neighbouring bases in a standard B-DNA geometry.

Coupling elements between consecutive intrastrand bases and interstrand Watson–Crick base pairs are compiled in Tables 5 and 6, respectively. They range, in absolute value, from 50 to 500 cm^{-1}, with a mean value close to 250 cm^{-1}; interstrand Watson–Crick and intrastrand nearest-neighbour coupling elements exhibit matching values.

The average magnitude of these elements gives interesting hints on the localised or delocalised behaviour of excitations in a double-stranded DNA fragment. For example, the first transitions of guanosine and cytidine are separated by 170 cm^{-1}; whereas coupling elements between these transitions amount to 130 and 300 cm^{-1} for intrastrand and interstrand geometries, respectively. As a consequence, excited states of $(dGdC)_n \cdot (dGdC)_n$ tracts are expected to be rather delocalised on, at least, these two monomers. Adenosine and thymidine $S_0 \rightarrow S_1$ transitions are distant of 790 cm^{-1}, whereas inter and intrastrand coupling elements are roughly 200 cm^{-1}. Broadening of the bands around the monomer transitions may grossly be considered equal to four times the coupling (800 cm^{-1}), so that the upper limit of the

Table 5
Dipolar coupling V (cm^{-1}) calculated using the atomic transition charges for intrastrand nearest neighbours; rise 3.4 Å; twist 36°

Transition 1	Transition 2	V
dA $S_0 \rightarrow S_1$	dA $S_0 \rightarrow S_1$	170
	dA $S_0 \rightarrow S_2$	93
	dT $S_0 \rightarrow S_1$	148
	dG $S_0 \rightarrow S_1$	−323
	dG $S_0 \rightarrow S_2$	−106
	dC $S_0 \rightarrow S_1$	86
dA $S_0 \rightarrow S_2$	dA $S_0 \rightarrow S_1$	256
	dA $S_0 \rightarrow S_2$	405
	dT $S_0 \rightarrow S_1$	−68
	dG $S_0 \rightarrow S_1$	−202
	dG $S_0 \rightarrow S_2$	−401
	dC $S_0 \rightarrow S_1$	418
dT $S_0 \rightarrow S_1$	dA $S_0 \rightarrow S_1$	231
	dA $S_0 \rightarrow S_2$	543
	dT $S_0 \rightarrow S_1$	217
	dG $S_0 \rightarrow S_1$	68
	dG $S_0 \rightarrow S_2$	−500
	dC $S_0 \rightarrow S_1$	215
dG $S_0 \rightarrow S_1$	dA $S_0 \rightarrow S_1$	−46
	dA $S_0 \rightarrow S_2$	180
	dT $S_0 \rightarrow S_1$	−451
	dG $S_0 \rightarrow S_1$	380
	dG $S_0 \rightarrow S_2$	−177
	dC $S_0 \rightarrow S_1$	133
dG $S_0 \rightarrow S_2$	dA $S_0 \rightarrow S_1$	−245
	dA $S_0 \rightarrow S_2$	−380
	dT $S_0 \rightarrow S_1$	48
	dG $S_0 \rightarrow S_1$	227
	dG $S_0 \rightarrow S_2$	375
	dC $S_0 \rightarrow S_1$	−409
dC $S_0 \rightarrow S_1$	dA $S_0 \rightarrow S_1$	14
	dA $S_0 \rightarrow S_2$	264
	dT $S_0 \rightarrow S_1$	−90
	dG $S_0 \rightarrow S_1$	127
	dG $S_0 \rightarrow S_2$	−214
	dC $S_0 \rightarrow S_1$	329

Table 6
Dipolar coupling V (cm^{-1}) calculated using the atomic transition charges for Watson–Crick base pairs

Transition 1	Transition 2	V
dT $S_0 \rightarrow S_1$	dA $S_0 \rightarrow S_1$	248
	dA $S_0 \rightarrow S_2$	266
dC $S_0 \rightarrow S_1$	dG $S_0 \rightarrow S_1$	306
	dG $S_0 \rightarrow S_2$	−243

adenosine $S_0 \rightarrow S_1$ and the lower limit of the thymidine $S_0 \rightarrow S_1$ bands are almost degenerate. Hence, the localised or delocalised behaviour of an

excitation in $(dAdT)_n \cdot (dAdT)_n$ sequences is more difficult to predict, and requires taking into account not only nearest-neighbours matrix elements but all other possible interactions.

5. Exciton states of double-stranded helices

In this section, we focus on two double-stranded helices $(dA)_{20} \cdot (dT)_{20}$ and $(dAdT)_{10} \cdot (dAdT)_{10}$. The properties of their exciton states are determined using the atomic transition charges model. The exciton matrix is built as described in Section 2 considering all possible interactions and taking into account the S_1 and S_2 states of adenosine and S_1 state of thymidine. Diagonalisation of the matrix yields 60 eigenstates whose oscillator strengths and delocalisation behaviour are discussed.

Fig. 6 shows the oscillator strengths associated with the eigenstates of each one of the double helices studied. As can be seen for both oligonucleotides, the global oscillator strength is smeared over a small number of states which are globally distributed into two narrow bands for $(dA)_{20} \cdot (dT)_{20}$ (around 37 750 and 39 750 cm^{-1}) and three narrow bands for $(dAdT)_{10} \cdot (dAdT)_{10}$ (around 37 600, 38 750 and 39 500 cm^{-1}). It is noteworthy that the most intense transition of each system shares the same eigenstate index $\langle 57 \rangle$. A general blue shift of the transition energies compared to those of the individual molecules is observed, with the high-energy region of the spectra bearing the major part of the intensity. Low-energy states are associated with negligible oscillator strength.

Since more than one chromophore transition has been considered to build the exciton matrix, delocalisation of the eigenstates may be subdivided into two categories: transition-governed delocalisation (e.g., delocalisation over a specific transition of one type of chromophore), and spatial delocalisation.

Fig. 7 presents the contribution of each of the three types of chromophore transitions to the eigenstates of the double helices, for which three energy regions can be distinguished. Eigenstates with low energies are mostly localised on the first transition of adenosine. The first transition of thymidine is the major contributor to eigenstates
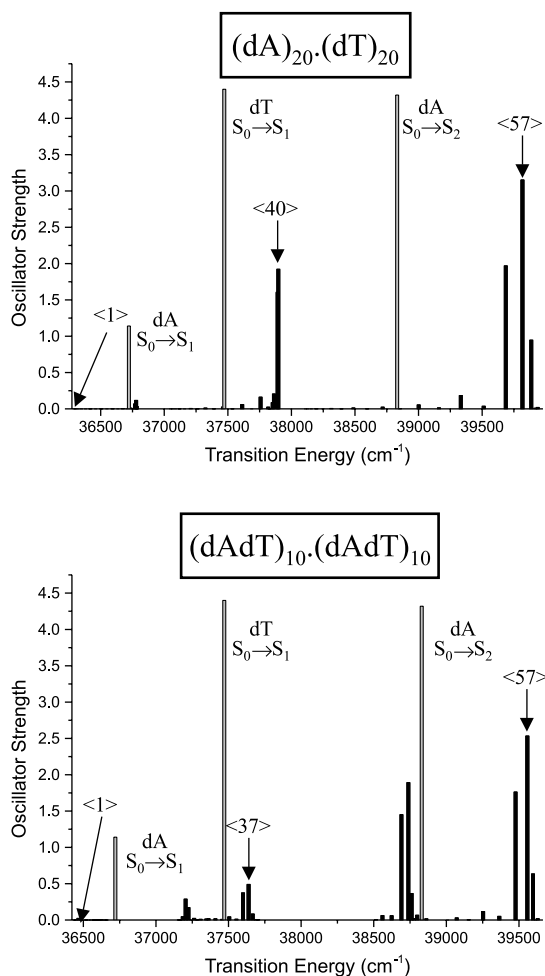

Fig. 6. Oscillator strengths associated with the eigenstates of the double-stranded eicosamers $(dA)_{20} \cdot (dT)_{20}$ and $(dAdT)_{10} \cdot (dAdT)_{10}$ as a function the corresponding energies. The grey columns designate the position of the transitions of individual chromophores. The arrows denote the eigenstates whose topography is shown in Fig. 9.

in the second region. Finally, high-energy eigenstates are mainly built on the second transition of adenosine. Borders between these three regions are clearly defined, so that contributions from a given transition can vary tremendously from one eigenstate to the next in the corresponding energy interval. This is particularly clear for $(dA)_{20} \cdot (dT)_{20}$; $(dAdT)_{10} \cdot (dAdT)_{10}$ shows a similar, albeit somewhat more complex, trend. This base sequence effect may be related to differences
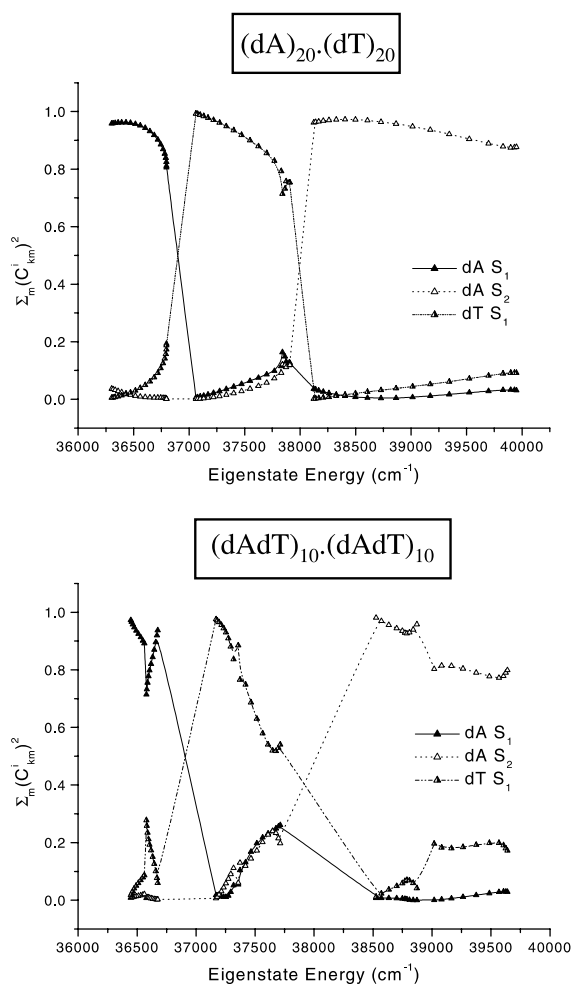
Fig. 7. Contribution of the S_1 state of thymidine and the S_1 and S_2 states of adenosine to the eigenstates of the of double-stranded eicosamers $(dA)_{20} \cdot (dT)_{20}$ and $(dAdT)_{10} \cdot (dAdT)_{10}$ as a function the eigenstate energy.

between corresponding matrix elements: in $(dA)_{20} \cdot (dT)_{20}$ transition-governed delocalisation occurs through intrastrand nearest-neighbour coupling, while in $(dAdT)_{10} \cdot (dAdT)_{10}$ it rests on the interstrand coupling between molecules in consecutive Watson–Crick base pairs. The latter type of coupling ($\approx 100 \ cm^{-1}$), although smaller than the former (around $250 \ cm^{-1}$), is still large enough to induce delocalisation of the excitation. Hence, our model predicts excitation delocalisation in both oligonucleotides to be governed by

the type of monomer transition. This implies localisation of the excitation on one strand in $(dA)_{20} \cdot (dT)_{20}$ and on the two strands in $(dAdT)_{10} \cdot (dAdT)_{10}$. A simplified explanation of this localisation behaviour may be attempted by considering the three exciton bands associated with each of the three chromophore transitions separately. For both systems examined, these bands do not overlap and the difference between their centres is larger than the maximum coupling values between the two corresponding transitions.

The plot of the participation ratio $1/L_k$, denoting the number of coherently coupled chromophores, versus the eigenstate index k, is presented in Fig. 8. We can see that the $1/L_k$ values found for $(dAdT)_{10} \cdot (dAdT)_{10}$ lie between 14 and 24, whereas those calculated for $(dAdT)_{10} \cdot (dAdT)_{10}$ range between 12 and 28, showing a considerable spatial extent of all eigenstates. It has been shown [71], in the case of helical columnar aggregates consisting of n identical chromophores, that the maximum value of the normalised participation ratio $1/nL_k$ is 0.7. In our case, the arrangement of one type of nucleoside within the double helix can be viewed as a one-dimensional aggregate. Hence, perfect spatial delocalisation over this system is expected to be characterised by a participation index of 14 (0.7×20). The fact that the majority of the eigenstates show participation ratios larger than 14 proves that they extend over both adenosine and thymidine chromophores. This is also quite apparent in Fig. 8: eigenstates located at the frontier between two regions (as appearing in Fig. 7) show a higher participation ratio, indicating contributions from more than one type of monomer transition. Mixing between adenosine and thymidine transitions in $(dAdT)_{10} \cdot (dAdT)_{10}$ appears more pronounced than in $(dA)_{20} \cdot (dT)_{20}$, with frontier eigenstates presenting participation ratios up to 29.

Finally, we focus on the delocalisation properties of a few remarkable eigenstates of the two oligomers, each belonging to one of the three energy regions depicted in Fig. 7. The topography of these eigenstates, e.g., the relative contribution of individual chromophores, is schematised in Fig. 9. The contribution of a given chromophore is rep-

$(dA)_{20} \cdot (dT)_{20}$

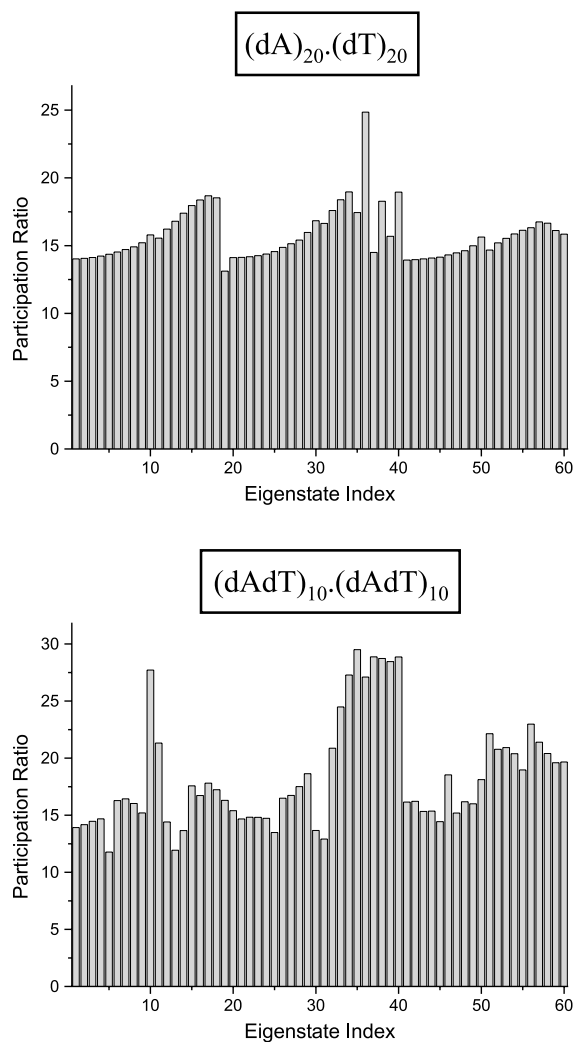
$(dAdT)_{10} \cdot (dAdT)_{10}$

Fig. 8. Participation ratio of the eigenstates of the double-stranded eicosamers $(dA)_{20} \cdot (dT)_{20}$ and $(dAdT)_{10} \cdot (dAdT)_{10}$ as a function the eigenstate index.

resented upwards or downwards, depending on the strand to which it belongs.

The first eigenstate, important to fluorescence studies, is concentrated almost exclusively on the first transition of the adenosine chromophores for both double-stranded DNA fragments. This implies a delocalisation on a single strand for $(dA)_{20} \cdot (dT)_{20}$ and on the two strands for $(dAdT)_{10} \cdot (dAdT)_{10}$. Similarly, eigenstate $\langle 57 \rangle$, bearing the highest oscillator strength in both systems, is mostly based on the adenosine $S_0 \rightarrow S_2$ transition,

although contributions from thymidine are no longer negligible. Finally, the mixing of the excited states of adenosine and thymidine is more substantial in eigenstates $\langle 40 \rangle$ of $(dA)_{20} \cdot (dT)_{20}$ and $\langle 37 \rangle$ of $(dAdT)_{10} \cdot (dAdT)_{10}$, which are also characterised by important oscillator strengths. All six eigenstates are distributed over the whole extent of the double helix.

6. Summary and comments

In the present communication, we have discussed problems related to the description of the electronic excited states and excitation transport in DNA double helices. In particular, we have pointed out how such studies can be improved using presently available experimental and computational techniques and the new methodologies which may result from their combination. The work reported here is our first step towards establishing a deeper understanding of phenomena which have significant biological interest.

The starting point of our study was the determination of the energies and transition moments of the lowest dipolar transitions of the individual chromophores forming the double helices. To this end, we recorded the absorption spectra of dilute $(10^{-5}$ M) water solutions of the four standard deoxynucleosides and decomposed them on the basis of fluorescence anisotropy and circular dichroism measurements reported in the literature. In parallel, we calculated these properties with the CS–INDO–CIPSI method. The agreement between the experimental and computed data was satisfactory for all the electronic transitions considered, i.e. $S_0 \rightarrow S_1$ for cytidine and thymidine, $S_0 \rightarrow S_1$ and $S_0 \rightarrow S_2$ for adenosine and guanosine.

Subsequently, we calculated the dipolar coupling for some typical stacked and paired dimers, using the atomic transition charge distribution model. We showed that neither the point dipole nor the extended dipole approximations provide a correct description of the dipolar coupling within double helices.

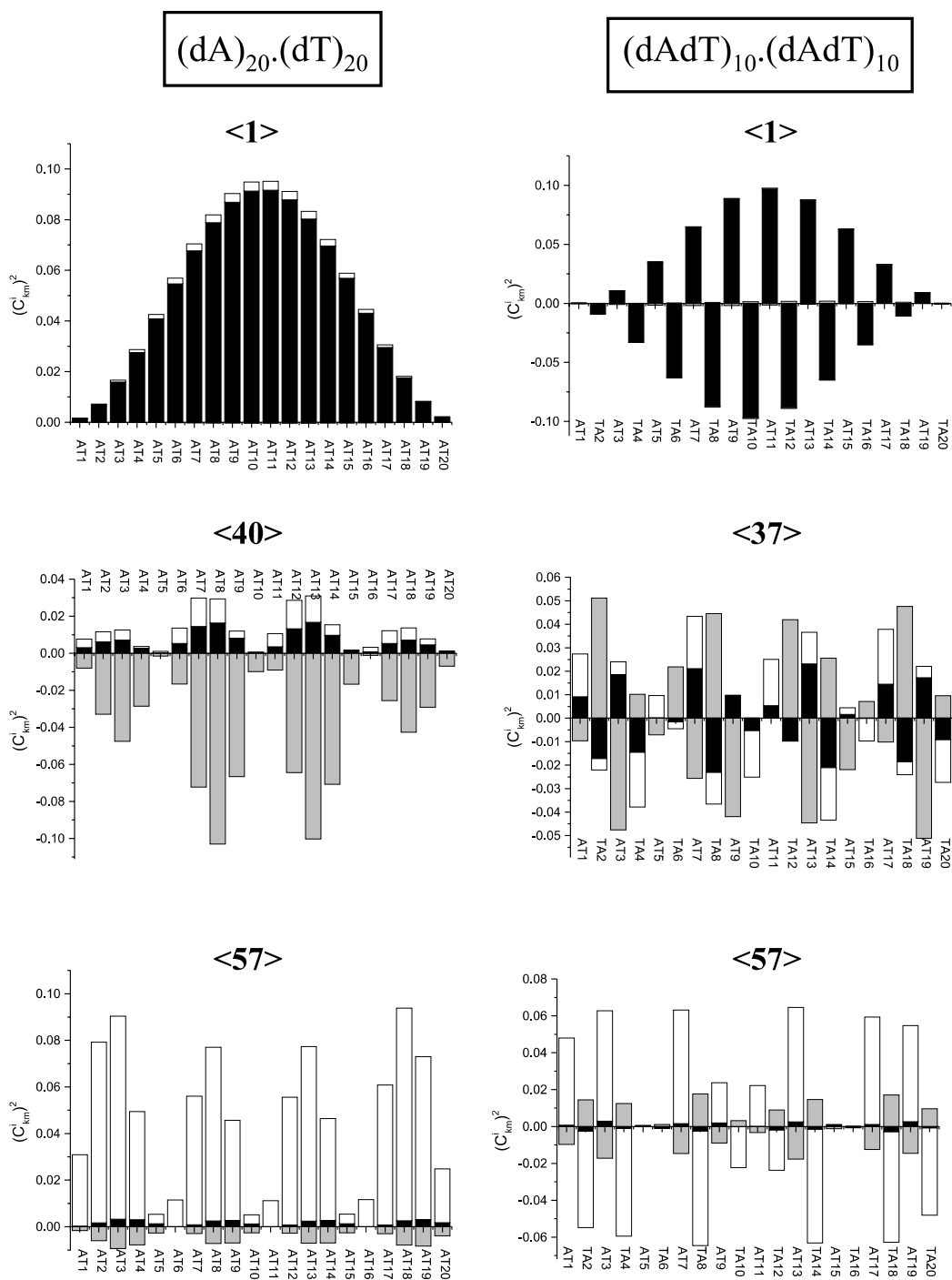Finally, we calculated the properties of the exciton states of two particular helical oligonucleo-

Fig. 9. Topography of three typical eigenstates of the double-stranded eicosamers $(dA)_{20} \cdot (dT)_{20}$ and $(dAdT)_{10} \cdot (dAdT)_{10}$: the lowest in energy ($\langle 1 \rangle$), those bearing the highest oscillator strength ($\langle 57 \rangle$) and two intermediate ones ($\langle 40 \rangle$ and $\langle 37 \rangle$). The coefficients ($C_{k,m}^i$) represent the contribution of chromophore m in its ith excited state (S_1 of adenosine in black, S_2 of adenosine in white, S_1 of thymidine in grey) to eigenstate k. The upper and lower parts of each histogram refer to chromophores located on each of the two strands.

tides, $(dA)_{20} \cdot (dT)_{20}$ and $(dAdT)_{10} \cdot (dAdT)_{10}$, considering three closely lying molecular electronic transitions, two for adenosine and one for thymidine. We found that the oscillator strength is distributed over a small number of eigenstates. All eigenstates are spatially delocalised over the whole length of the double helix. Most of them are built mainly on a single molecular state, but some, in particular in $(dAdT)_{10} \cdot (dAdT)_{10}$, result from the mixing of all three molecular states considered. A more thorough mixing of the excited states of the two nucleosides is expected in $(dG)_n \cdot (dC)_n$ and $(dGdC)_n \cdot (dGdC)_n$ tracts, since individual transitions of guanosine and cytidine lie much closer to each other than those of adenosine and thymidine.

The most important conclusion of our numerical calculations is that dipolar coupling alone may lead to a spatial delocalisation of the excitation within double helices having an idealised B-DNA geometry.

Prior to any comparison with experimental observations, we must take three important effects into account, which could notably reduce the spatial delocalisation of the electronic excitation found in the present study. Firstly, we need to model the site-dependent excitation energies originating from variations of the permanent dipole moment between the ground and the excited states [38]. Secondly, we must consider the plasticity of the double strands, by modelling solvent and temperature effects. We intend to reach both these goals by combining quantum chemistry calculations and molecular dynamics simulations both in the ground and in the excited states [32]. Thirdly, we have to include interactions due to orbital overlap, in particular the charge resonance and charge transfer terms, for which we are currently developing a new methodology. In parallel, we are also pursuing our experimental studies, making a particular effort to work only with well-defined molecular systems.

Acknowledgements

References

[1] (a) D.E. Brash, W.A. Haseltine, Nature 298 (1982) 189;
(b) J. Cadet, M. Berger, T. Douki, B. Morin, S. Raoul, J.-L. Ravanat, S. Spinelli, Biol. Chem. 378 (1997) 1275.

[2] (a) C. Chaozhi, T. Fiebig, O. Schiemann, J.K. Barton, A.H. Zewail, Proc. Natl. Acad. Sci. 97 (2000) 14052;
(b) A.A. Voityuk, J. Jortner, M. Bixon, N. Rösch, J. Chem. Phys. 114 (2001) 5614, and references therein.

[3] M. Guéron, J. Eisinger, R.G. Shulman, J. Chem. Phys. 47 (1967) 4077.

[4] D.M. Rayner, A.G. Szabo, R.O. Loutfy, R.W. Yip, J. Phys. Chem. 84 (1980) 289.

[5] S. Georghiou, S. Zhu, R. Weidner, C.-R. Huang, G. Ge, J. Biomol. Struct. Dyn. 8 (1990) 657.

[6] G. Ge, S. Georghiou, Photochem. Photobiol. 54 (1991) 301.

[7] S. Georghiou, G.R. Phillips, G. Ge, Biopolymers 32 (1992) 1417.

[8] C.-R. Huang, S. Georghiou, Photochem. Photobiol. 56 (1992) 95.

[9] I. Tinoco Jr., J. Am. Chem. Soc. 82 (1960) 4785.

[10] W. Rhodes, J. Am. Chem. Soc. 83 (1961) 3609.

[11] I. Tinoco Jr., R.W. Woody, D.F. Bradley, J. Chem. Phys. 38 (1963) 1317.

[12] T. Miyata, S. Yomosa, J. Phys. Soc. Jpn. 27 (1969) 720.

[13] J. Eisinger, R.G. Shulman, Science 161 (1968) 1311.

[14] T. Förster, Disc. Faraday Soc. 27 (1959) 7.

[15] G.H. Beaven, E.R. Holiday, E.A. Johnson, in: E. Chargaff, J.N. Davidson (Eds.), The Nucleic Acids, vol. 1, Academic Press, New York, 1955, p. 493.

[16] D. Voet, W.B. Gratzer, R.A. Cox, P. Doty, Biopolymers 1 (1963) 193.

[17] R.W. Wilson, P.R. Callis, J. Phys. Chem. 80 (1976) 2280.

[18] P.R. Callis, Ann. Rev. Phys. Chem. 34 (1983) 329.

[19] A. Holmén, A. Broo, B. Albinsson, B. Nordén, J. Am. Chem. Soc. 119 (1997) 12240.

[20] T.M. Nordlund, D. Xu, K.O. Evans, Biochemistry 32 (1993) 12090.

[21] D. Xu, T.M. Nordlund, Biophys. J. 78 (2000) 1042.

[22] G.D. Scholes, K.P. Ghiggino, J. Phys. Chem. 98 (1994) 4580.

[23] S. Marguet, D. Markovitsi, P. Millié, H. Sigal, S. Kumar, J. Phys. Chem. B 102 (1998) 4697.

[24] R. Silbey, Ann. Rev. Phys. Chem. 27 (1976) 203.

[25] G.D. Scholes, R.D. Harcourt, G.R. Fleming, J. Phys. Chem. B 101 (1997) 7302.

[26] D. Markovitsi, S. Marguet, L.K. Gallos, H. Sigal, P. Millié, P. Argyrakis, H. Ringsdorf, S. Kumar, Chem. Phys. Lett. 306 (1999) 163.

[27] M. Guéron, R.G. Shulman, J. Eisinger, Proc. Natl. Acad. Sci. 56 (1966) 814.

[28] T. Montenay-Garestier, C. Hélène, A.M. Michelson, Biochim. Biophys. Acta 182 (1969) 342.

[29] J.P. Morgan, M. Daniels, Photochem. Photobiol. 31 (1980) 207.

[30] J.P. Ballini, P. Vigny, M. Daniels, Biophys. Chem. 18 (1983) 61.

[31] S. Georghiou, S.M. Kubala, C.C. Large, Photochem. Photobiol. 67 (1998) 526.

[32] B. Hartmann, R. Lavery, Q. Rev. Biophys. 29 (1996) 309.

[33] P. Vigny, C.R. Acad. Sc. Paris t272 (1971) 3206.

[34] D.N. Nikogosyan, D. Angelov, B. Soep, L. Lindqvist, Chem. Phys. Lett. 252 (1996) 322.

[35] T. Häupl, C. Windolph, T. Jochum, O. Brede, R. Hermann, Chem. Phys. Lett. 280 (1997) 520.

[36] A. Reuther, H. Iglev, R. Laenen, A. Laubereau, Chem. Phys. Lett. 325 (2000) 360.

[37] J.-M.L. Pecourt, J. Peon, B. Kohler, J. Am. Chem. Soc. 122 (2000) 9348.

[38] C. Ecoffet, D. Markovitsi, P. Millié, J.P. Lemaistre, Chem. Phys. 177 (1993) 629.

[39] D. Markovitsi, S. Marguet, J. Bondkowski, S. Kumar, J. Phys. Chem. B 105 (2001) 1299.

[40] A.A. Voityuk, N. Rösch, M. Bixon, J. Jortner, J. Phys. Chem. B 104 (2000) 9740.

[41] V. Czikklely, H.D. Forsterling, H. Kuhn, Chem. Phys. Lett. 6 (1970) 207.

[42] D.B. Siano, D.E. Metzler, J. Chem. Phys. 51 (1969) 1856.

[43] J. Frenkel, Phys. Rev. 37 (1931) 1276.

[44] A.S. Davydov, Theory of Molecular Excitons, Plenum Press, New York, 1971.

[45] E.I. Rashba, M.D. Sturge, in: V.M. AgranovitchA.A. Maradudin (Eds.), Excitons, North-Holland, Amsterdam, 1982.

[46] H.C. Longuet-Higgins, Proc. R. Soc. London A 235 (1956) 537.

[47] P. Claverie, in: B. Pullman (Ed.), Intermolecular Interactions—From Diatomics to Biopolymers, Wiley, New York, 1978, p. 69.

[48] J.A. Pople, D.L. Beveridge, P.A. Dobosh, J. Chem. Phys. 47 (1967) 2026.

[49] P. Dean, Rev. Mod. Phys. 44 (1972) 127.

[50] M. Schreiber, Y. Toyozawa, J. Phys. Soc. Jpn. 51 (1982) 1537.

[51] M. Weissbluth, Q. Rev. Biophys. 4 (1971) 1.

[52] E. Brown, E.S. Pysh, J. Chem. Phys. 56 (1972) 31.

[53] A. Broo, A. Holmén, J. Phys. Chem. A 101 (1997) 3589.

[54] O. Kennard, W.N. Hunter, in: W. Saenger (Ed.), Nucleic Acids, Landolt-Börnstein New Series, vol. VII/1a, Springer, Berlin, 1989, p. 255.

[55] R.E. Dickerson, M. Bansal, C.R. Calladine, S. Diekmann, W.N. Hunter, O. Kennard, R. Lavery, H.C.M. Nelson, W.K. Olson, W. Saenger, Z. Shakked, H. Sklenar, D.M. Soumpasis, C.-S. Tung, E. von Kitzing, A.H.-J. Wang, V.B. Zhurkin, J. Mol. Biol. 205 (1989) 787.

[56] S. Arnott, E. Selsing, J. Mol. Biol. 88 (1974) 509.

[57] M.A. Viswamitra, Z. Shakked, P.G. Jones, G.M. Sheldrick, S.A. Salisbury, O. Kennard, Biopolymers 21 (1982) 513.

[58] A. Germain, P. Millié, Chem. Phys. 219 (1997) 265.

[59] H. DeVoe, I. Tinoco, J. Mol. Biol. 4 (1962) 518.

[60] R.F. Stewart, N. Davidson, J. Chem. Phys. 39 (1963) 255.

[61] L.B. Clark, J. Am. Chem. Soc. 99 (1977) 3934.

[62] P.R. Callis, W.T. Simpson, J. Am. Chem. Soc. 92 (1970) 3593.

[63] A. Volosov, Int. J. Quant. Chem. 36 (1989) 473.

[64] A. Volosov, R.W. Woody, J. Phys. Chem. 96 (1992) 4845.

[65] D. Theiste, P.R. Callis, R.W. Woody, J. Am. Chem. Soc. 113 (1991) 3260.

[66] J.D. Petke, G.M. Maggiora, R.E. Christoffersen, J. Am. Chem. Soc. 112 (1990) 5452.

[67] J. Lorentzon, M.P. Fülscher, B.O. Roos, J. Am. Chem. Soc. 117 (1995) 9265.

[68] B.O. Roos, M.P. Fülscher, P.Å. Malmqvist, M. Merchán, L. Serrano-Andrés, in: S.R. Langhoff (Ed.), Quantum Mechanical Electronic Structure Calculations with Chemical Accuracy, Kluwer, Dordrecht, 1995, p. 420.

[69] M.P. Fülscher, B.O. Roos, J. Am. Chem. Soc. 117 (1995) 2089.

[70] T. Miyata, H. Suzuki, S. Yomosa, J. Phys. Soc. Jpn. 25 (1968) 1428.

[71] D. Markovitsi, L.K. Gallos, J.P. Lemaistre, P. Argyrakis, Chem. Phys. 269 (2001) 147.